Synthesis of FeNi 3 Alloyed Nanoparticles by Hydrothermal Reduction

ARTICLE *in* THE JOURNAL OF PHYSICAL CHEMISTRY B · AUGUST 2006

Impact Factor: 3.3 · DOI: 10.1021/jp0625154 · Source: PubMed

3 AUTHORS, INCLUDING:

Rina Tannenbaum
Stony Brook University
143 PUBLICATIONS **3,157** CITATIONS

SEE PROFILE

Synthesis of $FeNi_3$ Alloyed Nanoparticles by Hydrothermal Reduction

Qilong Liao,[†,‡] Rina Tannenbaum,[‡] and Zhong Lin Wang*[,‡]

School of Materials Science and Engineering, Southwest University of Science and Technology, Mianyang 621010, China, and School of Materials Science and Engineering, Georgia Institute of Technology, Atlanta, Georgia 30332-0245

Received: April 24, 2006; In Final Form: May 29, 2006

The present paper presents a facile and low-cost hydrothermal method to synthesize stoichiometric $FeNi_3$ alloy nanoparticles by reducing $Ni(NO_3)_2{\cdot}6H_2O$ and $Fe(NO_3)_2{\cdot}9H_2O$ with hydrazine hydrate in strong alkaline media. X-ray diffraction patterns of as-prepared samples synthesized at 180 °C for different hydrothermal reaction times reveal that the products are pure stoichiometric $FeNi_3$ alloyed nanoparticles with well-defined crystalline cubic structure when the hydrothermal time is above 2 h, while no crystal phases are detected in the product obtained under ambient pressure in an open system from the same starting prescription. Transmission electron microscopic images show that the size of the as-prepared nanoparticles increases with prolongation of the hydrothermal reaction time. The as-prepared sample has the symmetric hysteresis loop behavior of ferromagnetic materials.

1. Introduction

There is considerable technological and theoretical interest in magnetic nanoparticles because properties such as magnetic recording density, recording speed, the noise suppression, and the material lifetime are remarkably enhanced with the decrease in magnetic particle size.[1] Transition metal alloys and compounds have been studied extensively in the past several decades for their increasing utility in electronic and energy conversion devices.[2] As important transition metal alloys, iron−nickel alloys are of great interest due to their useful magnetic properties.[3] These materials are important for applications as well as for fabrication. Iron−nickel alloy ultrafine particles can be prepared by a number of methods such as the mechanical attrition of elemental powders,[4] the levitation melting technique in a cryogenic environment of liquid nitrogen,[5] and electrodeposition in a flow cell.[6] Recently, nonstoichiometric iron−nickel nanometer-scale alloys were systematically investigated for a large range of compositions.[7] Bose and co-workers reported that stoichiometric nanocrystalline $FeNi_3$ particles can be synthesized within a silica gel matrix through wet chemical methods consisting of the reduction of their respective salts with hydrogen.[8]

Chemical reduction in solution has been widely used as the method of choice for the synthesis of nanometer-scale metallic powders because of the ease by which the process takes place.[9] However, as to the preparation of iron and its alloyed nanocrystals by this method, it still remains a challenge because iron salts readily hydrolyze and transform into stable hydroxides, which are very difficult to reduce.[10] The reduction of iron ions by KBH_4 in aqueous solution produces various compounds, such as $Fe_{65}B_{35}$, rather than pure metal or metal alloy nanoparticles.[11] Hydrazine hydrate has been successfully used as reducing agent for the syntheses of a variety of nanoscale metal materials because it has a strong reducing ability, has a low concentration of impurities, and is low cost. It was employed to prepare iron and Ni−Cu alloy nanocrystallites through a hydrothermal method.[12] The hydrothermal process appears to be a very effective method for preparing alloyed nanoparticles in a controlled manner because it allows for an almost simultaneaous reduction of two metal salts under high temperature and high pressure, conditions under which aqueous solutions exhibit a critical or supercritical state.[13]

In the present work, we describe a facile hydrothermal method to synthesize stoichiometric $FeNi_3$ alloy nanoparticles by reducing iron and nickel salts with hydrazine hydrate in strong alkaline media. The as-prepared powders were characterized by conventional techniques such as X-ray diffraction and transmission electron microscopy.

2. Experimental Section

The synthesis of stoichiometric iron−nickel alloy nanoparticles was performed in a 22-mL Teflon-lined stainless steel autoclave. All the reactants, $Ni(NO_3)_2{\cdot}6H_2O$ (98%, Alfa), $Fe(NO_3)_2{\cdot}9H_2O$ (98%, Alfa), hydrazine hydrate ($N_2H_4{\cdot}H_2O$, 80%, Aldrich), and NaOH (96%, Aldrich), were of reagent grade and used without further purification. In a typical experiment, a solution was first prepared by dissolving $Ni(NO_3)_2{\cdot}6H_2O$ and $Fe(NO_3)_2{\cdot}9H_2O$ in distilled water in amounts corresponding to the molar ratio of nickel to iron of 3:1. Subsequently, some NaOH was added to the solution to keep its pH around 11. A 2 mL volume of $N_2H_4{\cdot}H_2O$ was added to the solution as reductant, and 0.5 mL of sodium dodecyl sulfate (SDS) was used as surfactant. The mixture was stirred vigorously until it was homogeneous and then was transferred into an autoclave. The autoclave was sealed and put into a furnace, which was preheated to 180 °C. After heating for different times, the autoclave was taken out and cooled naturally to room temperature. The product was washed with distilled water and ethanol several times to remove impurities before the characterizations.

X-ray powder diffraction (XRD) patterns were collected on a Philips X-ray diffractometer with Cu Kα radiation (λ = 0.154 439 nm). Transmission electron microscopy (TEM) was performed on Hitachi JEOL 100C (at 100 kV) and HF2000 (at

* Corresponding author. E-mail: zhong.wang@mse.gatech.edu.
† Southwest University of Science and Technology.
‡ Georgia Institute of Technology.

10.1021/jp0625154 CCC: $33.50
Published on Web 06/28/2006

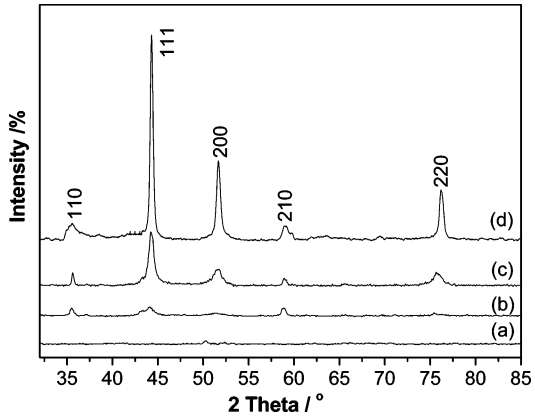

Figure 1. XRD patterns of samples prepared under different conditions: (a) at 70 °C for 10 h in an open system; (b) at 180 °C for 2 h in autoclave; (c) at 180 °C for 5 h in autoclave; (d) at 180 °C for 15 h in autoclave.

200 kV) transmission electron microscopes. The chemical composition of the as-synthesized powders was analyzed by energy-dispersive X-ray (EDX) spectroscopy equipped on the Hitachi HF2000 TEM. Magnetic properties were measured using a commercial superconducting quantum interference device (SQUID) magnetometer from the SPEC (CEA-Saclay, France) with a maximum applied field of 14 kOe.

3. Results and Discussion

The phase composition of as-synthesized powders was characterized by XRD, and the XRD patterns of samples are shown in Figure 1. The XRD patterns b, c, and d in Figure 1 correspond to products with the initial Ni:Fe molar ratio of 3:1 obtained at 180 °C for 2, 5, and 15 h, respectively. All peaks of the products can be indexed to stoichiometric $FeNi_3$ alloy (JCPDS 65-3244) with cubic structure. No iron and nickel oxides or hydroxides or other impurity phases are detected. The strong and sharp peaks and very low backgrounds reveal that the as-synthesized iron−nickel alloy particles had a high degree of crystallinity. The broadening of the diffraction peaks indicates that the samples are nanosize. The peak width decreases with the increase of hydrothermal holding time in the autoclave, which indicates that the sizes of the products increase with the increase in the reaction time. Nanoparticles generated following 2, 5, and 15 h residence time in the autoclave had average sizes of approximately 20, 30, and 70 nm, respectively. These were calculated from the half-width of the peaks of the XRD patterns, using the Scherrer formula.[14]

In our synthesis system, the iron and nickel salts were reduced by hydrazine hydrate in concentrated basic media. The reactions could be formulated as the following equations:

$$2Fe^{2+} + 4OH^- + N_2H_4 \rightarrow 2Fe + N_2 + 4H_2O, \quad E_0 = 0.44\ V \quad (1)$$

$$2Ni^{2+} + 4OH^- + N_2H_4 \rightarrow 2Ni + N_2 + 4H_2O, \quad E_0 = 0.49\ V \quad (2)$$

Here, E_0 stands for the standard electromotive force of reaction.[15] Metallic iron and metallic nickel give an intermetallic phase:

$$Fe + 3Ni \rightarrow FeNi_3 \quad (3)$$

During the course of the reaction, the reduction of iron and nickel ions will be effectively achieved by N_2H_4, which is a potent reducing agent in alkali solution.

In theory, the value of E_0 indicates that the fabrication of iron and nickel by the reduction of iron and nickel salt with hydrazine is feasible process. Nevertheless, if the reaction is maintained under ambient pressure in an open system, no iron−nickel particles can be produced. The XRD pattern in Figure 1a for the sample obtained at 70 °C for 10 h under ambient pressure shows that the product consists of noncrystalline powders, and no iron, nickel, or iron−nickel alloy nanoparticles are detected. This indicates that the hydrazine hydrate is not capable of reducing the iron and nickel salts in an open system in hot alkali solution. The disproportionation reaction of hydrazine hydrate in hot alkali solution could be expressed according to the following formula:[16]

$$3N_2H_4 \rightarrow N_2 + 4NH_3, \quad E_0 = 1.05\ V \quad (4)$$

It is obvious that the driving force for the occurrence of reaction 4 is much higher than that of the reactions in eqs 1 and 2, as evidenced by the different E_0 values of these reactions. Consequently, under normal atmospheric pressure, the disproportionation reaction of hydrazine constitutes the predominant reaction due to its higher E_0, limiting the efficiency of this compound as a reducing agent for Fe^{2+} and Ni^{2+} precursor salts. However, when the experiment is transferred into the closed system, the gas products of reaction 4 are kept in the autoclave, generating a relatively high partial pressure of nitrogen and ammonia. When this pressure rises to a critical value, it causes the reaction to become self-hindering, i.e., it limits the occurrence of the disproportionation reaction, and hence allows reactions 1 and 2 to take place and, in time, become dominant.

Figure 2 shows the TEM images of stoichiometric $FeNi_3$ alloys obtained at different conditions. Figure 2a reveals the morphology of nanoparticles formed at 180 °C for 2 h. Figure 2b shows the morphology of nanoparticles obtained at 180 °C for 5 h, revealing 20−30 nm sheetlike particles, in agreement with the sizes calculated by using the Scherrer formula. Figure 2c shows nanoparticles whose diameters are 70−100 nm, obtained at 180 °C for 15 h. It is quite obvious that the morphologies of the products change considerably as a function of the residence time in the autoclave. On the basis of the morphologies observed by TEM, it can be concluded that the sizes of the particles increase with the increase of reaction time, a fact that is consistent with the results of the XRD patterns.

The select area electron diffraction (SAED) pattern (Figure 3c) taken from the as-prepared $FeNi_3$ nanoparticles (Figure 3a) synthesized at 180 °C for 15 h consists of a number of rings and some distinct spots along the ring contours, suggesting a cubic polycrystalline structure. The rings in an electron diffraction pattern arise due to the diffracted electron beam from a set of lattice planes in the crystallites present in the sample satisfying the Bragg diffraction condition. In other words, the ring is an envelope of all diffracted spots. Along some of the rings a few spots appear to be prominent, which indicates the formation of crystallites. The interplanar spacing values are calculated from Bragg's diffraction equation using the diffraction ring diameter and the camera length of the transmission electron microscope. The calculated results indicate that the five diffraction rings, from the inner to the outer direction in Figure 3c, correspond to the (110), (111), (200), (210), and (220) crystal planes, respectively, which is similar to the diffraction pattern of stoichiometric $FeNi_3$ alloy that is reported by JCPDS 65-3244, with a cell parameter $a = 3.552$.

To confirm the chemical composition of the as-prepared nanoparticles, energy-dispersive X-ray spectroscopy (EDS) was performed on the HF 2000 TEM. Figure 3b shows EDS spectra

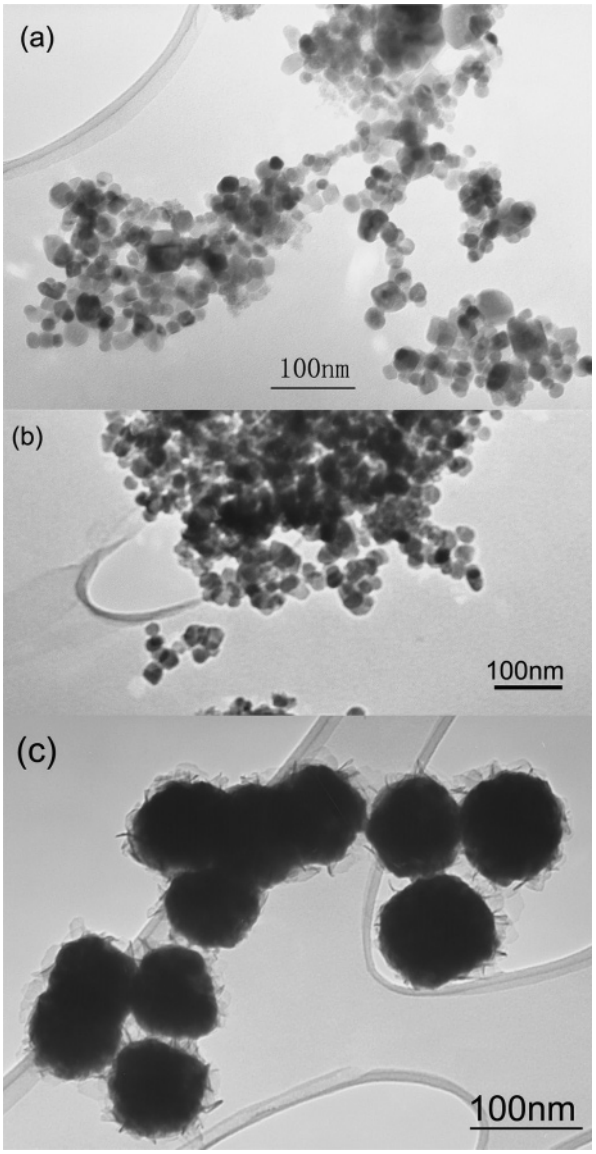

Figure 2. TEM images of $FeNi_3$ synthesized at 180 °C for (a) 2, (b) 5, and (c) 15 h in autoclave.

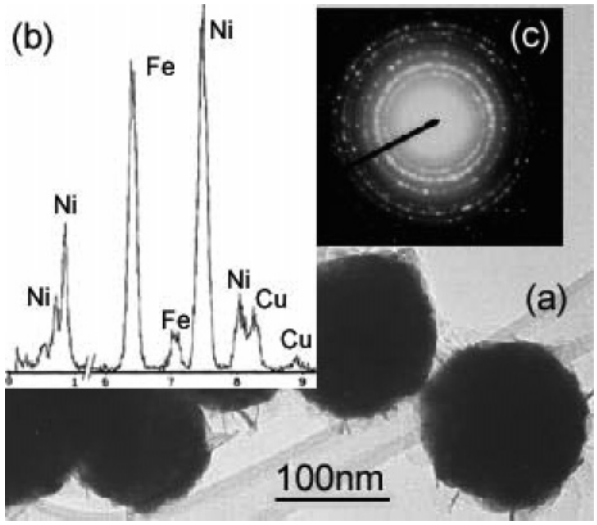

Figure 3. (a) HFTEM image of $FeNi_3$ alloy; (b) EDS pattern from the $FeNi_3$ alloy, showing the presence of Fe and Ni in the structure; (c) SAED spectroscopy of $FeNi_3$ alloy.

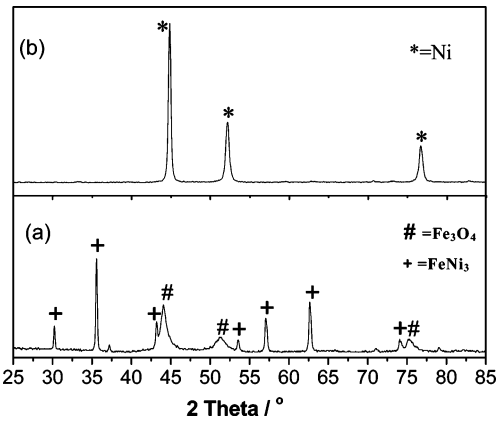

Figure 4. XRD patterns for the products prepared at 180 °C for 15 h with different initial Ni:Fe ratios: (a) initial Ni:Fe ratio 2:1; (b) initial Ni:Fe ratio 4:1.

taken from the as-prepared nanoparticles (Figure 3a) at 180 °C for 15 h. The only detectable elements by EDS from the as-prepared nanoparticles are iron and nickel, and the corresponding elementary analysis reveals that the atomic ratio of nickel to iron is 3:1. This supports the XRD and SAED results that the as-synthesized products are $FeNi_3$ nanoparticle crystals.

To investigate the influence of the initial Ni:Fe molar ratio of starting materials on the formation of the products, we synthesized several samples with different initial molar ratios of starting materials at 180 °C for 15 h. The XRD pattern reveals that stoichiometric $FeNi_3$ nanoparticles can be obtained only from the reaction with the initial Ni:Fe molar ratio of 3:1 (see Figure 1d). Figure 4a shows that some Fe_3O_4 and $FeNi_3$ can be simultaneously obtained when the initial Ni:Fe molar ratio is 2:1. The formation of Fe_3O_4 is due to the oxidation of excessive metallic iron reduced by hydrazine during the course of hydrothermal reaction and the relative lack of enough metallic nickel in the system to form a more stable Fe−Ni alloy phase. Figure 4b shows that only metallic nickel can be detected when the initial Ni:Fe molar ratio is 4:1. A possible explanation for this result is that Ni^{2+} can be reduced by hydrazine easier than Fe^{2+} in hydrous solution.[10] By the time iron would nucleate in a substantial fashion, the reaction in the autoclave would have been already terminated. Hence, iron will exist in the final mixture mainly as unreacted salt, which would be subsequently washed out with the solution upon separation of the nanocrystallites.

To measure the magnetic properties of the as-synthesized $FeNi_3$ alloy nanoparticles, the hysteresis loop curve for the sample synthesized at 180 °C for 15 h was measured by a SQUID magnetometer at room temperature. Figure 5 shows the hysteresis loop of as-synthesized $FeNi_3$ alloy nanoparticles. It indicates that the sample has the symmetric hysteresis loop behavior of ferromagnetic materials and its coercive force is 87.12 Oe.

4. Conclusions

In summary, stoichiometric $FeNi_3$ alloyed nanoparticles have been successfully synthesized through a hydrothermal method in strong alkaline solution by reduction of $Ni(NO_3)_2 \cdot 6H_2O$ and $Fe(NO_3)_2 \cdot 9H_2O$ salts with hydrazine hydrate at 180 °C for the reaction time range of 2−15 h. The gas pressure formed in the hydrothermal system could inhibit the decomposition of hydrazine and be favorable for the reactions between hydrazine and Fe^{2+} or Ni^{2+}, which result in the creation of a intermetallic Fe−Ni phase. XRD patterns reveal that the products are pure stoichiometric $FeNi_3$ alloy nanoparticles with well-defined crystalline cubic structure when the hydrothermal time is above

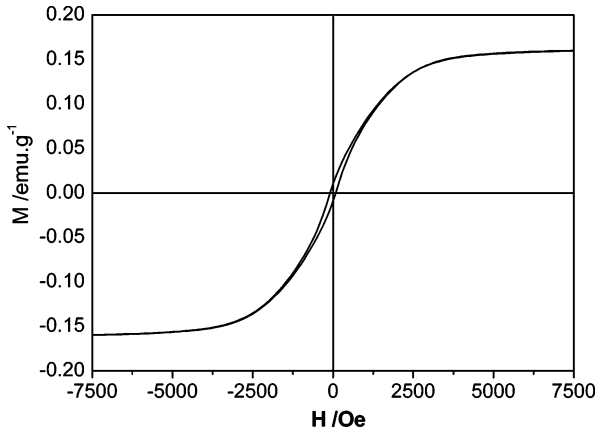

Figure 5. Hysteresis loop at room temperature on the sample prepared at 180 °C for 15 h.

2 h, while no crystal phases are detected in the product obtained under ambient pressure in an open system. TEM images indicate that the size of the as-prepared nanoparticles increases with prolongation of the hydrothermal reaction time. The as-prepared nanoparticles have polycrystalline structure and are composed of only iron and nickel elements, which are demonstrated by SAED pattern and EDX spectroscopy. The hysteresis loop reveals that the sample has the symmetric hysteresis loop behavior of ferromagnetic materials and its coercive force is 87.12 Oe. This work provides a simple, effective, and low-cost synthetic method to prepare stoichiometric $FeNi_3$ alloy nanoparticles.

Acknowledgment. The work was supported by National Nature Science Foundation of China (NSAF Joint Fund project, No. 10476024) and NSF (DMR 9733160).

References and Notes

(1) Li, X. G.; Chiba, A.; Takahashi, S. *J. Magn. Magn. Mater.* **1997**, *170*, 339.

(2) Tremel, W.; Kleinke, H.; Derstroff, V.; Reisner, C. *J. Alloys Compd.* **1995**, *219*, 73.

(3) Datta, A.; Pal, M.; Chakravorty, D.; Das, D.; Chintalapudi, S. N. *J. Magn. Magn. Mater.* **1999**, *205*, 301.

(4) Kuhrt, C.; Schultz, L. *J. Appl. Phys.* **1993**, *73*, 1975.

(5) Zhou, Y. H.; Harmelin, M.; Bigot, J. *Mater. Sci. Eng.* **1991**, *A133*, 775.

(6) Kima, S. H.; Sohn, H. J.; Joo, Y. C.; Kim, Y. W.; Yim, T. H.; Lee, H. Y.; Kang, T. *Surf. Coat. Technol.* **2005**, *199*, 43.

(7) Liu, Q. F.; Wang, J. B.; Yan, Z. J.; Xue, D. S. *Phys. Rev. B* **2005**, *72*, 44412.

(8) Bose, P.; Bid, S.; Pradhan, S. K.; Pal, M.; Chakravorty, D. *J. Alloys Compd.* **2002**, *343*, 192.

(9) Shpan'ko, S. P.; Grigor'ev, V. P.; Dymnikova, O. V.; Burlov, A. S. *Prot. Met.* **2005**, *41*, 541.

(10) Su, X. B.; Zheng, H. G.; Yang, Z. P.; Zhu, Y. C.; Pan, A. L. *J. Mater. Sci.* **2003**, *38*, 4581.

(11) Corrias, A.; Ennas, G. *Chem. Mater.* **1993**, *5*, 1722.

(12) Niu, H. L.; Chen, Q. W.; Lin, Y. S.; Jia, Y. S.; Zhu, H. F.; Ning, M. *Nanotechnology* **2004**, *15*, 1054.

(13) Zhong, Z. T.; Biom, D. A.; Gai, Z.; Thompson, J. R.; Shan, J.; Dai, S. *J. Am. Chem. Soc.* **2003**, *125*, 7528.

(14) Wagner, C. W. J.; Aqua, E. N. *Adv. X-ray Anal.* **1964**, *7*, 46.

(15) Yu, K.; Kim, D. J.; Chung, H. S.; Liang, H. Z. *Mater. Lett.* **2003**, *57*, 3992.

(16) Ni, X. M.; Su, X. B.; Zheng H. G.; Zhang D.; Yang, D. D.; Zhao, Q. B. *J. Cryst. Growth* **2005**, *275*, 548.